
CMS Physics Analysis Summary

Contact: cms-pag-conveners-b2g@cern.ch

2015/12/15

Search for W' boson resonances decaying into a top quark and a bottom quark in the leptonic final state at $\sqrt{s} = 13$ TeV

The CMS Collaboration

Abstract

We present a search for the production of a heavy gauge boson W' decaying into a top quark and a bottom quark. The dataset used corresponds to an integrated luminosity of 2.2 fb^{-1} collected by the CMS experiment at $\sqrt{s} = 13 \text{ TeV}$. The final state signature searched for is lepton (e, μ) plus jets and missing transverse energy. We find no evidence of a W' and set 95% confidence level (C.L.) upper limits on its production cross-section times branching fraction. For W' bosons with purely right handed couplings, the observed (expected) 95% C.L. lower limit is 2.38 (2.17) TeV. These are currently the most stringent limits in this channel.

1 Introduction

Massive charged gauge bosons, usually called W' , are predicted by several extensions of the Standard Model [1–5]. In many models, the W' bosons couple more strongly to the third generation than to the first and second generations [6, 7], motivating searches in the decay channel $W' \rightarrow tb$ ($t\bar{b} + \bar{t}b$). Such searches have been performed at the Tevatron [8, 9] and at the LHC [10–12].

This note updates the analysis presented in Ref. [10] using data collected by the CMS experiment [13] at $\sqrt{s} = 13$ TeV. Although the integrated luminosity at $\sqrt{s} = 13$ TeV is currently smaller than that at $\sqrt{s} = 8$ TeV, the W' production cross-section is larger by nearly an order of magnitude for a W' boson with a mass of 2 TeV. Following Ref. [10], we analyze the lepton (e, μ) plus jets and missing transverse energy (E_T^{miss}) final state resulting from the decay chain $W' \rightarrow tb$, $t \rightarrow bW \rightarrow bl\nu$. We focus on W' bosons with purely right-handed couplings and widths narrow compared to their masses.

2 Signal and Background Modeling

The signal modeling is similar to that used in Ref. [10] except that only right-handed W' bosons (W'_R) are simulated. The simulated signal is produced using COMPHEP 4.5.2rc10 [14] for W' boson masses between 1 and 3 TeV at intervals of 100 GeV. The factorization scale is set to the mass of the W' boson. The leading order (LO) cross-section is taken from COMPHEP and scaled to the next to leading order (NLO) cross-section using a k -factor of 1.2 [15, 16]. W' production cross-sections range from 3.15 pb at 1 TeV to 0.013 pb at 3 TeV.

The principal features of leptonic $W' \rightarrow tb$ decays are a high- p_T lepton, significant E_T^{miss} arising from the neutrino and two high- p_T b-jets. The main sources of backgrounds for such final states are $t\bar{t}$, W +jets, single-top (tW, s-, and t-channel), Z/γ^* +jets, dibosons (WW, WZ and ZZ) and the continuum multijet background. Monte-Carlo samples for Z/γ^* +jets, s-, and t-channel single-top and W +jets are generated using MadGraph5_aMC@NLO [17], $t\bar{t}$ and single-top in the tW channel are generated using POWHEG [18] and all other backgrounds are generated using PYTHIA [19].

All simulated signal and background samples are processed through PYTHIA for parton fragmentation and hadronization. The simulation of the CMS detector is performed by GEANT [20]. All simulated samples include additional proton-proton interactions (pile-up) weighted such that the number of interactions agrees with that in the data. Additional correction factors derived from the data are applied to leptons, jets and E_T^{miss} to ensure agreement with the data.

3 Object and Event Selection

All leptons, jets and E_T^{miss} used in this search are reconstructed using the Particle Flow algorithm [21]. Exactly one lepton is required to have fired a non-isolated trigger, be within the detector acceptance ($|\eta| < 2.5$ for electrons excluding the barrel-end cap transition region, and $|\eta| < 2.1$ for muons) and be associated with a reconstructed primary vertex. At 13 TeV, the top quark from the W' decay is more boosted than at 8 TeV, causing the b-jet and lepton decay products to be closer to each other. This results in isolation having a significant impact on signal efficiency so, unlike in Ref. [10], we do not require leptons to be isolated. Electrons and muons are required to satisfy $p_T > 180$ GeV and fulfill several identification criteria. Electron candidates are selected using a multivariate technique based on the shower-shape information, the

quality of the track, the match between the track and electromagnetic cluster, the fraction of total cluster energy in the hadronic calorimeter, the amount of activity in the surrounding regions of the tracker and calorimeters and the probability of the electron originating from a converted photon. The track associated with a muon candidate is required to have hits in the pixel and muon detectors, a good quality fit and a transverse impact parameter close to the beam spot. To reduce the multijet background, the selected lepton is required to satisfy $\Delta R(\text{lepton, nearest jet}) > 0.4$ or $p_T^{\text{rel}}(\text{muon, nearest jet}) > 50 \text{ GeV}$ or $p_T^{\text{rel}}(\text{electron, nearest jet}) > 60 \text{ GeV}$ where $\Delta R = \sqrt{\Delta\eta^2 + \Delta\phi^2}$ and p_T^{rel} is defined as the magnitude of the lepton momentum orthogonal to the jet axis. Events with additional charged leptons with $p_T > 35 \text{ GeV}$ and $|\eta| < 2.5$ for electrons and $|\eta| < 2.4$ for muons are vetoed.

Jets are clustered using the anti- k_T algorithm with a cone size of $\Delta R = 0.4$ [22] and are required to satisfy $p_T > 25 \text{ GeV}$ and $|\eta| < 2.4$. There must be at least two jets in the event and the p_T of the leading jet must be greater than 350 (450) GeV in the electron (muon) channel. The p_T of the sub-leading jet must be greater than 30 GeV. Since both jets are expected to come from bottom quarks, at least one jet is required to be b-tagged using the Combined Secondary Vertex algorithm with the Inclusive Vertex Finder. [23]

The E_T^{miss} is required to be above 50 GeV in the muon channel and 120 GeV in the electron channel. The requirement is higher for electrons due to a greater presence of the multijet background in this channel. To further reduce the multijet background, we also require $|\Delta\phi(E_T^{\text{miss}}, e)| < 2$ radians.

4 Event Reconstruction

The W' boson is notable for a resonance in the tb invariant mass that is narrow relative to the mass of the W' boson. The tb invariant mass can be reconstructed from the observed charged lepton, E_T^{miss} and jets in the event. The xy -components of the neutrino momentum are taken from the E_T^{miss} and the z -component is calculated by constraining the invariant mass of the lepton and neutrino to the W boson mass (80.4 GeV). This method leads to a quadratic equation in p_z^{ν} . In the case the two solutions are real numbers, both solutions are used to reconstruct W boson candidates. If both solutions contain imaginary parts, then we set p_z^{ν} to the real part of the solutions, and then recompute p_T^{ν} which yields another quadratic ambiguity. In this case, we use only the solution with the mass closest to 80.4 GeV.

Once we have assigned all components of the neutrino momentum, we combine the viable neutrino solutions with the charged lepton to create W boson candidate(s). We then reconstruct the top quark by combining the W candidates with each jet individually. Whichever jet yields a top quark mass closest to 172.5 GeV is labeled the “best jet” and is used to reconstruct the top quark. In the case of two W candidates, we only use the candidate which yields the best top mass. Finally, we combine the top candidate with the highest p_T jet which is not the “best jet”, yielding our reconstructed W' invariant mass.

Three final selection requirements are applied. In the muon channel, the reconstructed top quark mass must be consistent with the true top quark mass: $100 < m_{top} < 250 \text{ GeV}$. The p_T of the reconstructed top quark must satisfy $p_T^{\text{top}} > 250$ in both channels. Finally, the p_T of the combination of the two leading p_T jets must satisfy $p_T^{\text{jet1+jet2}} > 350 \text{ GeV}$. All of the selection requirements are optimized separately for the electron and muon channels. The invariant mass distributions after this final selection are shown in Figure 1. The event yields before and after this final selection are in Tables 1 and 2.

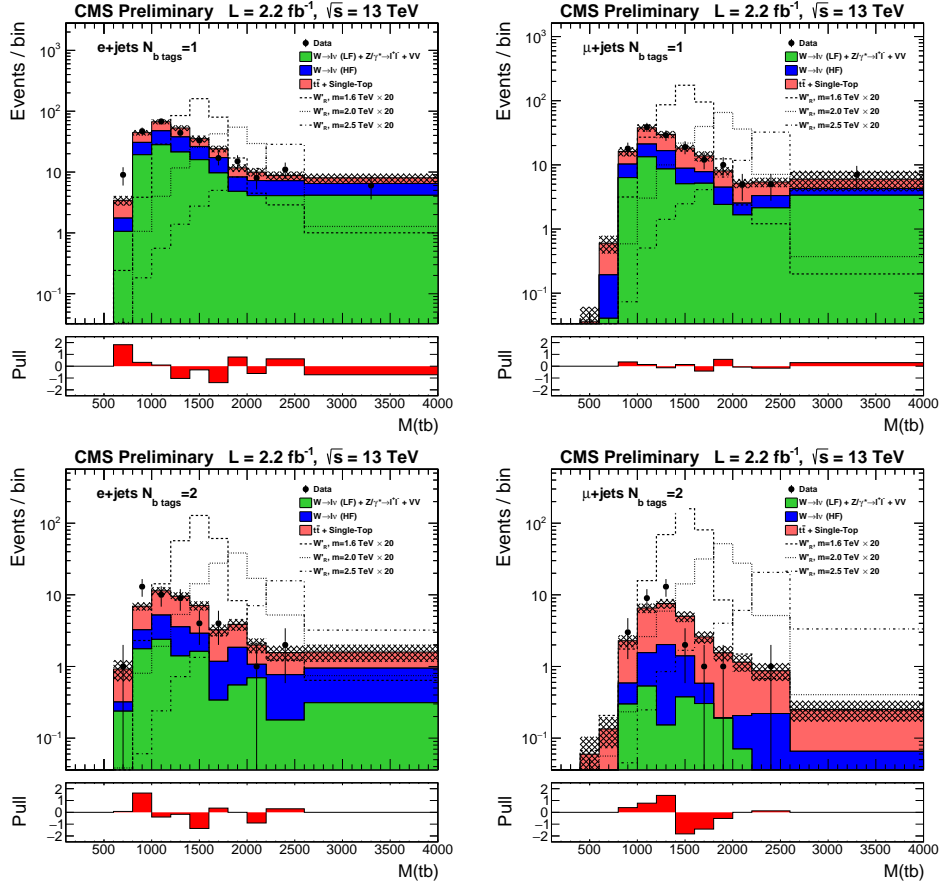


Figure 1: The reconstructed tb invariant mass distributions after the final selection for the electron (left) and muon (right) channels with 1 (top) and 2 (bottom) b-tagged jets. Uncertainties based on the shape of the distribution are not shown.

5 Background Estimation

All of the backgrounds used in this search are estimated using simulation with checks performed in control regions for $W+jets$ and top pair backgrounds to confirm that they are well-modeled. For $W+jets$, we verify the modeling of the flavor content using two samples which differ from the event selection only in b-tagging. The *pre b-tag* sample does not have any b-tagging requirements while the events in the *0 b-tag* sample must not have any b-tagged jets. The *0 b-tag* sample is used to derive a first order scale factor for light flavor $W+jets$. This scale factor is then applied to the $W+jets$ simulation, and then the difference in the *pre b-tag* distribution is used to calculate a first order $W+jets$ heavy flavor scale factor. This procedure is repeated until further iterations do not cause the calculated scale factors to shift by more than 0.1%. We also confirm this calculation by solving the system of equations resulting from the iteration analytically, and we find that the two methods yield identical results.

For the $t\bar{t}$ background, we verify the modeling of the transverse momentum of top quarks in the signal region. This check is performed in two $t\bar{t}$ -enriched regions: one which differs from the signal mainly in requiring $450 \text{ GeV} < M(\text{tb}) < 750 \text{ GeV}$ and one which removes the second lepton veto and instead requires an additional electron or muon with a p_T of at least 35 GeV. These checks show that there are still differences between the top p_T in data and in simulation so we reweight the $t\bar{t}$ background using the same empirical function as in Ref. [10].

Table 1: Number of selected data and background events in the muon channel. The expectation corresponds to an integrated luminosity of 2.2 fb^{-1} . "Final selection" refers to the additional cuts of $p_T^{top} > 250$, $p_T^{jet1+jet2} > 350$, and $250 < m_{top} < 250$. The quoted uncertainty does not include shape-based systematics.

Process	Number of Events					
	Object Selection				Final Selection	
	≥ 0 b-tags	$= 0$ b-tags	$= 1$ b-tags	$= 2$ b-tags	$= 1$ b-tags	$= 2$ b-tags
Data:	770	431	281	58	143	30
Background:						
$t\bar{t}$	124	36	64	25	46	16
tqb	7	2	4	1	3	1
tW	17	5	9	3	4	1
$\bar{t}W$	16	3	9	4	5	2
tb	1	0	0	0	0	0
$W(\rightarrow \ell\nu) + jj$	304	218	80	6	25	1
$W(\rightarrow \ell\nu) + bb/cc$	283	132	128	23	45	7
$Z(\rightarrow \ell\ell) + jets$	47	26	21	0	12	0
VV	20	17	3	0	0	0
Total Background	819 ± 60	439 ± 36	318 ± 24	62 ± 5	140 ± 11	28 ± 3

Table 2: Number of selected data and background events in the electron channel. The expectation corresponds to an integrated luminosity of 2.2 fb^{-1} . "Final selection" refers to the additional cuts of $p_T^{top} > 250$ and $p_T^{jet1+jet2} > 350$. The quoted uncertainty does not include shape-based systematics.

Process	Number of Events					
	Object Selection				Final Selection	
	≥ 0 b-tags	$= 0$ b-tags	$= 1$ b-tags	$= 2$ b-tags	$= 1$ b-tags	$= 2$ b-tags
Data:	802	435	309	58	256	44
Background:						
$t\bar{t}$	132	40	68	24	52	17
tqb	8	2	5	2	4	1
tW	22	5	11	6	10	5
$\bar{t}W$	20	4	11	4	9	4
tb	1	0	1	0	1	0
$W(\rightarrow \ell\nu) + jj$	359	262	89	8	77	7
$W(\rightarrow \ell\nu) + bb/cc$	306	146	139	22	119	18
$Z(\rightarrow \ell\ell) + jets$	9	8	3	-1	4	-1
VV	26	17	9	0	7	0
Total Background	883 ± 83	484 ± 50	336 ± 32	65 ± 7	283 ± 22	51 ± 5

6 Systematic Uncertainties

The systematic uncertainties for this analysis can be grouped into two categories: uncertainties on the overall normalization and uncertainties on the shape of the $M(t\bar{b})$ distribution. The normalization uncertainties include uncertainties on the integrated luminosity, theoretical cross sections and branching fractions, lepton identification and trigger efficiencies. The shape uncertainties consist mainly of the jet energy scale, the b-tagging efficiency and mistag rates and the Monte-Carlo generator-related uncertainties such as the Q^2 scale. The lepton and trigger uncertainties are derived from data using the tag-and-probe method whereas the uncertainties due to simulation are obtained by varying the relevant parameter at generator level. The calculation of the systematic uncertainty for the heavy flavor $W+jets$ background is based on the uncertainty in b-tagging. The systematic uncertainty due to pileup is calculated by varying the

minimum bias cross section by 5%. The uncertainty due to the top p_T reweighting is derived from the difference between applying the reweighting and performing the analysis without it. The uncertainties are listed in Table 3.

Table 3: Systematic uncertainties.

Source	Rate Uncertainty	Shape?
Luminosity	4.6%	No
Trigger Efficiency (e/μ)	4%/2%	No
Lepton ID Efficiency (e/μ)	5%/2%	No
Jet Energy Scale	$\pm\sigma(p_T, \eta)$	Yes
Jet Energy Resolution	$\pm\sigma(p_T, \eta)$	Yes
b/c -tagging	$\pm\sigma(p_T, \eta)$	Yes
light quark mis-tagging	$\pm\sigma(p_T, \eta)$	Yes
PDF	$\pm\sigma(p_T, \eta)$	Yes
Renormalization and factorization Q^2 scale	$2Q^2$ and $0.5Q^2$	Yes

7 Results

We use the invariant mass distributions from the background and signal samples to calculate the expected limits on the W' cross section times the branching ratio of $W' \rightarrow tb \rightarrow \ell\nu bb$ using the Bayesian statistics approach in the *theta* package [24]. The Bayesian approach uses a binned likelihood in order to calculate the upper limits on the signal production times branching fraction $\sigma(pp \rightarrow W') \times \mathcal{B}(W' \rightarrow tb)$. In order to increase sensitivity we separate the events into four independent categories before combining the results. Events are split by lepton type (electron or muon) and by the number of b-tagged jets out of the first two leading p_T jets (=1 or =2). In order to keep the statistical uncertainties small and simulated distributions smooth, we bin the tb invariant mass distribution as follows: 1 bin from 100 GeV to 400 GeV, 9 bins of width 200 GeV from 400 to 2200 GeV, 1 bin of width 400 GeV from 2200 to 2600 GeV, and 1 bin from 2600 to 4000 GeV. These distributions are used as input to the *theta* framework in calculating the limits. The expected and observed limits are shown in Figures 2 and 3.

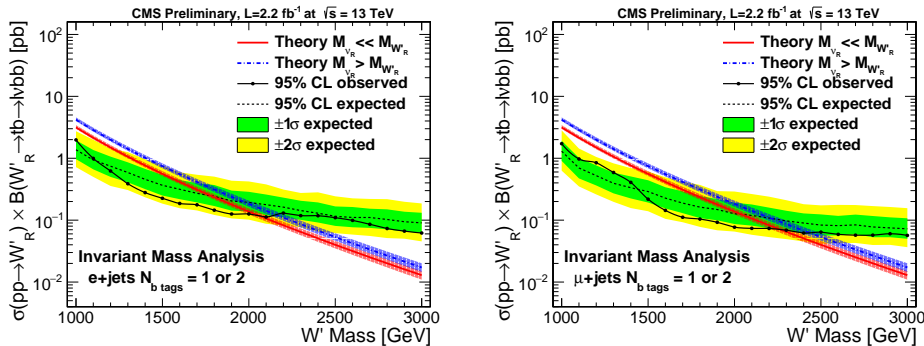


Figure 2: Expected and observed Bayesian 95% C.L. upper limits on the production cross-section of right-handed W' bosons in the electron+jets channel (left) and muon+jets channel (right) for combined 1 or 2 b-tags for right-handed W' bosons. W' masses with a cross-section exceeding the observed limit are excluded. Limits have been calculated with an integrated luminosity of 2.2 fb^{-1} .

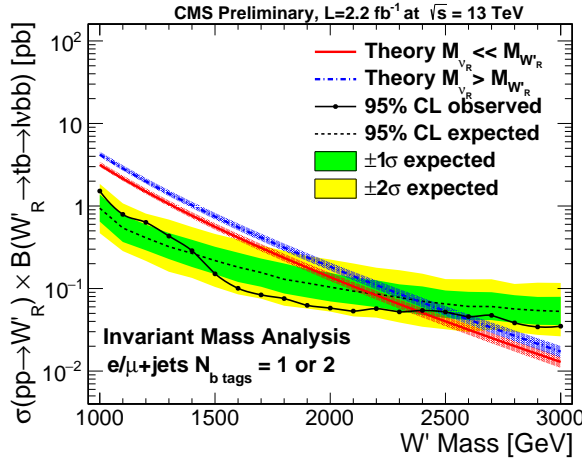


Figure 3: Expected and observed Bayesian 95% C.L. upper limits for all channels combined on the production cross-section of right-handed W' bosons. W' masses with a cross-section exceeding the observed limit are excluded. Limits have been calculated with an integrated luminosity of 2.2 fb^{-1} .

8 Conclusion

We have conducted a search for heavy W' bosons decaying to a top and bottom quark in proton-proton collisions at $\sqrt{s} = 13 \text{ TeV}$. We study the tb invariant mass distribution and find good agreement between the data and predictions from simulation. We find no evidence for W' boson production and set 95% C.L. upper limits on the production cross-section times branching fraction for $W' \rightarrow tb$. Comparing our measurement to the theoretical prediction for the nominal value of the cross-section, we find an observed (expected) limit of 2.38 (2.17) TeV. Despite the integrated luminosity at 13 TeV being an order of magnitude smaller, these limits already exceed their 8 TeV counterparts.

References

- [1] M. Schmaltz and D. Tucker-Smith, "LITTLE HIGGS THEORIES", *Annual Review of Nuclear and Particle Science* **55** (2005), no. 1, 229–270, doi:10.1146/annurev.nucl.55.090704.151502.
- [2] T. Appelquist, H.-C. Cheng, and B. A. Dobrescu, "Bounds on universal extra dimensions", *Phys. Rev. D* **64** (Jun, 2001) 035002, doi:10.1103/PhysRevD.64.035002.
- [3] H.-C. Cheng, C. T. Hill, S. Pokorski, and J. Wang, "Standard model in the latticized bulk", *Phys. Rev. D* **64** (Aug, 2001) 065007, doi:10.1103/PhysRevD.64.065007.
- [4] R. S. Chivukula, E. H. Simmons, and J. Terning, "Limits on noncommuting extended technicolor", *Phys. Rev. D* **53** (May, 1996) 5258–5267, doi:10.1103/PhysRevD.53.5258.
- [5] R. N. Mohapatra and J. C. Pati, "Left-right gauge symmetry and an 'isoconjugate' model of CP violation", *Phys. Rev. D* **11** (Feb, 1975) 566–571, doi:10.1103/PhysRevD.11.566.
- [6] D. J. Muller and S. Nandi, "Topflavor: a separate SU(2) for the third family", *Physics Letters B* **383** (1996), no. 3, 345 – 350, doi:10.1016/0370-2693(96)00745-9.
- [7] E. Malkawi, T. Tait, and C.-P. Yuan, "A model of strong flavor dynamics for the top quark", *Physics Letters B* **385** (1996), no. 14, 304 – 310, doi:10.1016/0370-2693(96)00859-3.
- [8] D0 Collaboration, "Search for W' Boson Resonances Decaying to a Top Quark and a Bottom Quark", *Phys. Rev. Lett.* **100** (May, 2008) 211803, doi:10.1103/PhysRevLett.100.211803. <http://link.aps.org/doi/10.1103/PhysRevLett.100.211803>.
- [9] D0 Collaboration, "Search for W' resonances with left- and right-handed couplings to fermions", *Physics Letters B* **699** (2011), no. 3, 145 – 150, doi:10.1016/j.physletb.2011.03.066. <http://www.sciencedirect.com/science/article/pii/S0370269311003510>.
- [10] CMS Collaboration, "Search for $W' \rightarrow tb$ decays in the lepton + jets final state in pp collisions at $\sqrt{s} = 8$ TeV", *JHEP* **05** (2014) 108, doi:10.1007/JHEP05(2014)108, arXiv:1402.2176.
- [11] ATLAS Collaboration, "Search for $W' \rightarrow t\bar{b}$ in the lepton plus jets final state in proton-proton collisions at a centre-of-mass energy of $\sqrt{s} = 8$ TeV with the ATLAS detector", *Phys. Lett.* **B743** (2015) 235–255, doi:10.1016/j.physletb.2015.02.051, arXiv:1410.4103.
- [12] ATLAS Collaboration, "Search for $W' \rightarrow tb \rightarrow qqbb$ decays in pp collisions at $\sqrt{s} = 8$ TeV with the ATLAS detector", *Eur. Phys. J.* **C75** (2015), no. 4, 165, doi:10.1140/epjc/s10052-015-3372-2, arXiv:1408.0886.
- [13] CMS Collaboration, "The CMS experiment at the CERN LHC. The Compact Muon Solenoid experiment", *J. Instrum.* **3** (2008) S08004. 361 p.

[14] CompHEP Collaboration, “CompHEP 4.4: Automatic computations from Lagrangians to events”, *Nucl. Instrum. Meth.* **A534** (2004) 250–259, doi:10.1016/j.nima.2004.07.096, arXiv:hep-ph/0403113.

[15] Z. Sullivan, “Fully differential W' production and decay at next-to-leading order in QCD”, *Phys.Rev.* **D66** (2002) 075011, doi:10.1103/PhysRevD.66.075011, arXiv:hep-ph/0207290.

[16] D. Duffty and Z. Sullivan, “Model independent reach for W -prime bosons at the LHC”, *Phys.Rev.* **D86** (2012) 075018, doi:10.1103/PhysRevD.86.075018, arXiv:1208.4858.

[17] J. Alwall et al., “The automated computation of tree-level and next-to-leading order differential cross sections, and their matching to parton shower simulations”, *JHEP* **07** (2014) 079, doi:10.1007/JHEP07(2014)079, arXiv:1405.0301.

[18] S. Frixione, P. Nason, and C. Oleari, “Matching NLO QCD computations with Parton Shower simulations: the POWHEG method”, *JHEP* **11** (2007) 070, doi:10.1088/1126-6708/2007/11/070.

[19] S. M. T. Sjostrand and P. Z. Skands, “PYTHIA 6.4 Physics and Manual”, *JHEP* **0605** (2006) doi:10.1088/1126-6708/2006/05/026.

[20] S. J. Allison et al. *IEEE Trans. Nucl. Sci.* **53** (2006) 270.

[21] CMS Collaboration, “Commissioning of the particle-flow event reconstruction with leptons from J/ψ and W decays at 7 TeV”, technical report, 2010.

[22] M. Cacciari, G. P. Salam, and G. Soyez, “The Anti- $k(t)$ jet clustering algorithm”, *JHEP* **0804** (2008) 063, doi:10.1088/1126-6708/2008/04/063, arXiv:0802.1189.

[23] CMS Collaboration, “Identification of b -quark jets with the CMS experiment”, *JINST* **8** (2013) P04013, doi:10.1088/1748-0221/8/04/P04013, arXiv:1211.4462.

[24] T. Müller, J. Ott, and J. Wagner-Kuhr, “theta - a framework for template-based modeling and inference”, http://www-ekp.physik.uni-karlsruhe.de/~ott/theta/testing/html/theta_auto_intro.html.